Benemérita Universidad Autónoma de Puebla

and

Dual C-P Institute of High Energy Physics, México

Meeting of the NExT Institute
Rutherford-Appleton Laboratory
March 20, 2013

Talk: Light charged Higgs boson phenomenology in 2HDM-III

Speaker: Jaime Hernández-Sánchez

1

Outline

- Brief introduction of 2HDM-III and how this version could contain the other versions of 2HDM.
- Flavor constraints from low energy processes
- Phenomenology of charged Higgs could be quiet different.
- Some interesting channels decays: $H+ \to cb, ts, W+\gamma, WZ$
- $cb \to H+ \to \tau\nu$ production mode
- $t \to b\, H+$ and $H+ \to cb$
- $cb \to H+ \to W+ h$ could it be testable with SM ?

Versions of the 2HDM

Type I: one Higgs doublet provides masses to all quarks (up- and down-type quarks) (~SM).

Type II: one Higgs doublet provides masses for up-type quarks and the other for down-type quarks (~MSSM).

Type III: the two doublets provide masses for up and down type quarks, as well as charged leptons.

We could consider this model as a generic description of physics at a higher scale (i. e. Radiative corrections of the MSSM Higgs sector* or from extradimension**).

*J. L. Díaz-Cruz, R. Noriega-Papaqui and A. Rosado, Phys. Rev. D 71, 015014 (2005).

**A. Aranda, J.L. Díaz-Cruz, J. Hernández-Sánchez, R. Noriega-Papaqui, Phys. Lett. B 658, 57 (2007).

Absence of (tree-level) FCNCs

→ constraints on Higgs couplings

In SM FCNC automatically absent as same operation diagonalising the mass matrix automatically diagonalises the Higgs-fermion couplings.

- There are three ways:
- (1) Discrete symmetries. This choice is based on the Glashow–Weinberg's theorem concerning FCNC's in models with several Higgs doublets.
  (MSSM: Y=-1 (+1) doublet copules to donw (up)-type fermion, as required by SUSY)
- (2) Radiative suppression. When a given set of Yukawa matrices are present at tree-level, but the other ones arise only as a radiative effect: i.e. the 2HDM-II, it is transformed into 2HDM-III through loops-effects of sfermions and gauginos.
- (3) Flavor symmetries. Suppression of FCNC effects can also be achieved when a certain form of the Yukawa matrices that reproduce the observed fermion masses and mixing angles is implemented in the model, i.e. THDM-III. (Yukawa textures)

J.L. Diaz-Cruz, R Noriega-Papaqui, A. Rosado. Phys. Rev. D69,095002 (2004)

Yukawa textures

The Yukawa textures are consistents with the relations between quarks masses and flavor mixing parameters.

Yukawa textures could come of a theory more fundamental and it could be a flavor symmetry.

H. Fritzsch, Z. Z. Xing, Prog.Part. Nucl. Phys. 45 (2000)1.
H. Fritzsch, Z. Z. Xing, Phys. Lett. 555 (2003)63.

Yukawa sector in 2HDM type III

$$\mathcal{L}_Y = Y_1^u \bar{Q}_L \Phi_1 u_R + Y_2^u \bar{Q}_L \Phi_2 u_R + Y_1^d \bar{Q}_L \Phi_1 d_R + Y_2^d \bar{Q}_L \Phi_2 d_R \,,$$

$$(\tilde{Y}_2^l)_{ij} = \frac{\sqrt{m_i m_j}}{v} \tilde{\chi}_{ij} = \frac{\sqrt{m_i m_j}}{v} \chi_{ij} e^{\vartheta_{ij}},$$

$$M_f = \frac{1}{\sqrt{2}}(v_1 Y_1^f + v_2 Y_2^f), \qquad f = u, d, l,$$

$$M_f = \begin{pmatrix} 0 & C_f & 0 \\ C_f^* & \tilde{B}_f & B_f \\ 0 & B_f^* & A_f \end{pmatrix}.$$

$$\bar{M}_f = V_{fL}^\dagger M_f V_{fR}.$$

Seesaw mechanism in MSSM

Flavor Violation among the Sleptons. In the leptonic sector, we begin with a Lagrangian:

$$-\mathcal{L} = \overline{E}_R Y_E L_L H_d + \overline{\nu}_R Y_\nu L_L + \tfrac{1}{2}\nu_R^\top M_R \nu_R \tag{1}$$

$$\begin{aligned}\frac{d}{d\log Q}(m_{\tilde{L}}^2)_{ij} &= \left(\frac{d}{d\log Q}(m_{\tilde{L}}^2)_{ij}\right)_{\mathrm{MSSM}} \\ &+ \frac{1}{16\pi^2}\left[m_{\tilde{L}}^2 Y_\nu^\dagger Y_\nu + Y_\nu^\dagger Y_\nu m_{\tilde{L}}^2 + 2(Y_\nu^\dagger m_{\tilde{\nu}_R}^2 Y_\nu + m_{H_u}^2 Y_\nu^\dagger Y_\nu + A_\nu^\dagger A_\nu)\right]_{ij}\end{aligned} \tag{2}$$

$$\left(\Delta m_{\tilde{L}}^2\right)_{ij} \simeq -\frac{\log(M/M_R)}{16\pi^2}\left(6m_0^2(Y_\nu^\dagger Y_\nu)_{ij} + 2\left(A_\nu^\dagger A_\nu\right)_{ij}\right) \tag{3}$$

where m_0 is a common scalar mass evaluated at the scale $Q = M$, and $i \neq j$. If we further assume that the A-terms are proportional to Yukawa matrices, then:

$$\left(\Delta m_{\tilde{L}}^2\right)_{ij} \simeq \xi\left(Y_\nu^\dagger Y_\nu\right)_{ij} \tag{4}$$

K.S. Babu, C. Kolda, Phys. Rev. Lett. 89,241802 (2002).

2HDM-III + Yukawa texture
contain the following information:

It could come from a more fundamental theory (susy models with seesaw mechanism).

+

Yukawa texture is the flavor symmetry of the model and do not require of the discrete flavor symmetry.

+

The Higgs potential must be expressed in the most general form.

T. P. Cheng, M. Sher, Phys. Rev. D33,11 (1987)
J.L. Diaz-Cruz, R Noriega-Papaqui, A. Rosado. Phys. Rev. D69,095002 (2004)

$$\mathcal{L}_{\text{yukawa}}^{\text{THDM}} = -\sum_{f=u,d,\ell}\left(\frac{m_f}{v}\xi_h^f\overline{f}fh + \frac{m_f}{v}\xi_H^f\overline{f}fH - i\frac{m_f}{v}\xi_A^f\overline{f}\gamma_5 fA\right)$$
$$-\left\{\frac{\sqrt{2}V_{ud}}{v}\overline{u}\left(m_u\xi_A^u\mathrm{P}_L + m_d\xi_A^d\mathrm{P}_R\right)d\,H^+ + \frac{\sqrt{2}m_\ell\xi_A^\ell}{v}\overline{\nu_L}\ell_R H^+ + \text{H.c.}\right\},$$

	ξ_h^u	ξ_h^d	ξ_h^ℓ	ξ_H^u	ξ_H^d	ξ_H^ℓ	ξ_A^u	ξ_A^d	ξ_A^ℓ
Type-I	c_α/s_β	c_α/s_β	c_α/s_β	s_α/s_β	s_α/s_β	s_α/s_β	$\cot\beta$	$-\cot\beta$	$-\cot\beta$
Type-II	c_α/s_β	$-s_\alpha/c_\beta$	$-s_\alpha/c_\beta$	s_α/s_β	c_α/c_β	c_α/c_β	$\cot\beta$	$\tan\beta$	$\tan\beta$
Type-X	c_α/s_β	c_α/s_β	$-s_\alpha/c_\beta$	s_α/s_β	s_α/s_β	c_α/c_β	$\cot\beta$	$-\cot\beta$	$\tan\beta$
Type-Y	c_α/s_β	$-s_\alpha/c_\beta$	c_α/s_β	s_α/s_β	c_α/c_β	s_α/s_β	$\cot\beta$	$\tan\beta$	$-\cot\beta$

TABLE II: The mixing factors in Yukawa interactions in Eq. (6)

Mayumi Aoki, Shinya Kanemura, Koji Tsumura, Kei Yagyu. Phys.Rev. D80 (2009) 015017

$$\mathcal{L}^{\bar{f}_i f_j H^+} = -\left\{ \frac{\sqrt{2}}{v} \overline{u}_i \left(m_{d_j} X_{ij} P_R + m_{u_i} Y_{ij} P_L \right) d_j \, H^+ + \frac{\sqrt{2} m_{\ell_j}}{v} Z_{ij} \overline{\nu_L} \ell_R H^+ + H.c. \right\}$$

$$X_{ij} = \sum_{l=1}^{3} (V_{\rm CKM})_{il} \left[X \frac{m_{d_l}}{m_{d_j}} \delta_{lj} - \frac{f(X)}{\sqrt{2}} \sqrt{\frac{m_{d_l}}{m_{d_j}}} \tilde{\chi}^d_{lj} \right],$$

$$Y_{ij} = \sum_{l=1}^{3} \left[Y \delta_{il} - \frac{f(Y)}{\sqrt{2}} \sqrt{\frac{m_{u_l}}{m_{u_i}}} \tilde{\chi}^u_{il} \right] (V_{\rm CKM})_{lj}.$$

$$Z^{\ell}_{ij} = \left[Z \frac{m_{\ell_i}}{m_{\ell_j}} \delta_{ij} - \frac{f(Z)}{\sqrt{2}} \sqrt{\frac{m_{\ell_i}}{m_{\ell_j}}} \tilde{\chi}^{\ell}_{ij} \right],$$

2HDM-III	X	Y	Z
like-2HDM-I	$-\cot\beta$	$\cot\beta$	$-\cot\beta$
like-2HDM-II	$\tan\beta$	$\cot\beta$	$\tan\beta$
like-2HDM-X	$-\cot\beta$	$\cot\beta$	$\tan\beta$
like-2HDM-Y	$\tan\beta$	$\cot\beta$	$-\cot\beta$

$$\left(g^{f_u i f_d j H^+}_{2HDM-III} = g^{f_u i f_d j H^+}_{2HDM-any} + \Delta g^{f_u i f_d j H^+} \right)$$

J. Hernandez-Sanchez, S. Moretti, R. Noriega-Papaqui, A. Rosado
arXiv: 1212.6818, submitted to JHEP

Some constraints of processes to below energy

$\mu - e$ *universality in* τ *decays*

$$\frac{BR(\tau \to \mu\bar{\nu}_\mu\nu_\tau)}{BR(\tau \to e\bar{\nu}_e\nu_\tau)}\frac{f(m_e^2/m_\tau^2)}{f(m_\mu^2/m_\tau^2} \simeq 1 + \frac{R^2}{4} - 0.25R.$$

$$R = \frac{m_\tau m_\mu}{M_{H^+}^2} Z_{33}\, Z_{22} \;=\; \frac{m_\tau m_\mu}{M_{H^+}^2}\left[Z - \frac{f(Z)}{\sqrt{2}}\chi_{33}^l\right]\left[Z - \frac{f(Z)}{\sqrt{2}}\chi_{22}^l\right].$$

$$\boxed{\frac{|Z_{22}Z_{33}|}{m_{H^\pm}^2} \leq 0.16\ GeV^{-1}}$$

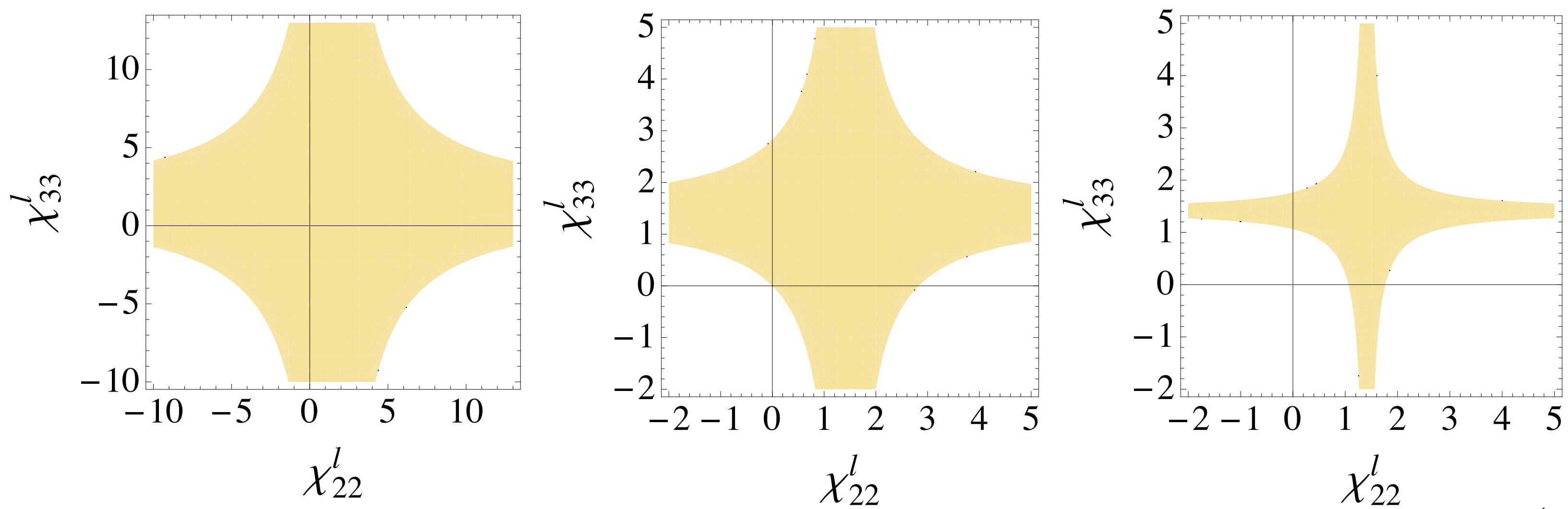

FIG. 1. Considering the constraint from $\mu - e$ universality in τ decays, we show the allowed region (orange color) for χ_{22}^l and χ_{33}^l when Z takes values of 10 (left-panel), 40 (center-panel) and 80 (right-panel). Here, 90 GeV $\leq m_{H^\pm} \leq$ 130 GeV.

J. Hernandez-Sanchez, S. Moretti, R. Noriega-Papaqui, A. Rosado
arXiv: 1212.6818, submitted to JHEP

10

We consider $D \to \mu\nu$, $B \to \tau\nu$, $D_s \to \mu\nu, \tau\nu$

$$\frac{B(M \to \ell\nu)}{B(M \to \ell\nu)_{SM}} = |1 - \Delta_{ij}|^2$$

$$\Delta_{ij} = \left(\frac{m_M}{m_{H^\pm}}\right)^2 Z\left(\frac{Y_{ij} m_{u_i} + X_{ij} m_{d_j}}{m_{u_i} + m_{d_j}}\right)$$

$$R_{B \to D\tau\nu} = a_0 + a_1(m_B^2 - m_D^2)\delta_{23} + a_2(m_B^2 - m_D^2)^2\delta_{23}^2,$$

$$\delta_{ij} = -\frac{Z_{33}}{m_{H^\pm}^2}\left(\frac{Y_{ij} m_{u_i} - X_{ij} m_{d_j}}{m_{u_i} - m_{d_j}}\right).$$

$R(D^*) = \mathbf{BR}(B \to D^*\tau\nu)/\mathbf{BR}(B \to D^* l\nu)$

$$R(D) = 0.44 \pm 0.058 \pm 0.042,$$
$$R(D^*) = 0.332 \pm 0.024 \pm 0.018.$$

can explain simultaneously

$$\mathrm{BR}(B \to X_s\gamma)_{NLO} = B_{SL} \left|\frac{V_{ts}^* V_{tb}}{V_{cb}}\right|^2 \frac{6\alpha_{em}}{\pi\theta(z)\kappa(z)} \left[|D|^2 + A + \Delta\right] ,$$

$$\delta C^{0,eff}_{(7,8)}(\mu_W) = \left|\frac{Y^u_{33} Y^{u*}_{32}}{V_{tb}V_{ts}}\right| C^0_{(7,8),YY}(y_t) + \left|\frac{X^u_{33} Y^{u*}_{32}}{V_{tb}V_{ts}}\right| C^0_{(7,8),XY}(y_t),$$

$$\left|\frac{Y_{33}Y^*_{32}}{V_{tb}V_{ts}}\right| = \left[\left(Y - \frac{f(y)}{\sqrt{2}}\chi^u_{33}\right) - \sqrt{\frac{m_c}{m_t}}\left(\frac{V_{cb}}{V_{tb}}\right)\frac{f(Y)}{\sqrt{2}}\chi^u_{23}\right]\left[\left(Y - \frac{f(y)}{\sqrt{2}}\chi^u_{33}\right) - \sqrt{\frac{m_c}{m_t}}\left(\frac{V_{cs}}{V_{ts}}\right)\frac{f(Y)}{\sqrt{2}}\chi^u_{23}\right]^*,$$

$$\left|\frac{X_{33}Y^*_{32}}{V_{tb}V_{ts}}\right| = \left[\left(X - \frac{f(X)}{\sqrt{2}}\chi^d_{33}\right) - \sqrt{\frac{m_s}{m_b}}\left(\frac{V_{ts}}{V_{tb}}\right)\frac{f(X)}{\sqrt{2}}\chi^d_{23}\right]\left[\left(Y - \frac{f(y)}{\sqrt{2}}\chi^u_{33}\right) - \sqrt{\frac{m_c}{m_t}}\left(\frac{V_{cs}}{V_{ts}}\right)\frac{f(Y)}{\sqrt{2}}\chi^u_{23}\right]^*,$$

$B^0 - \bar{B}^0$ **mixing**

$$\left|\frac{Y_{33}Y^*_{32}}{V_{tb}V_{ts}}\right| < 0.25, \qquad -1.7 < Re\left[\frac{X_{33}Y^*_{32}}{V_{tb}V_{ts}}\right] < 0.7.$$

$(80\ \mathrm{GeV} \le m_{H^\pm} \le 300\ \mathrm{GeV})$.

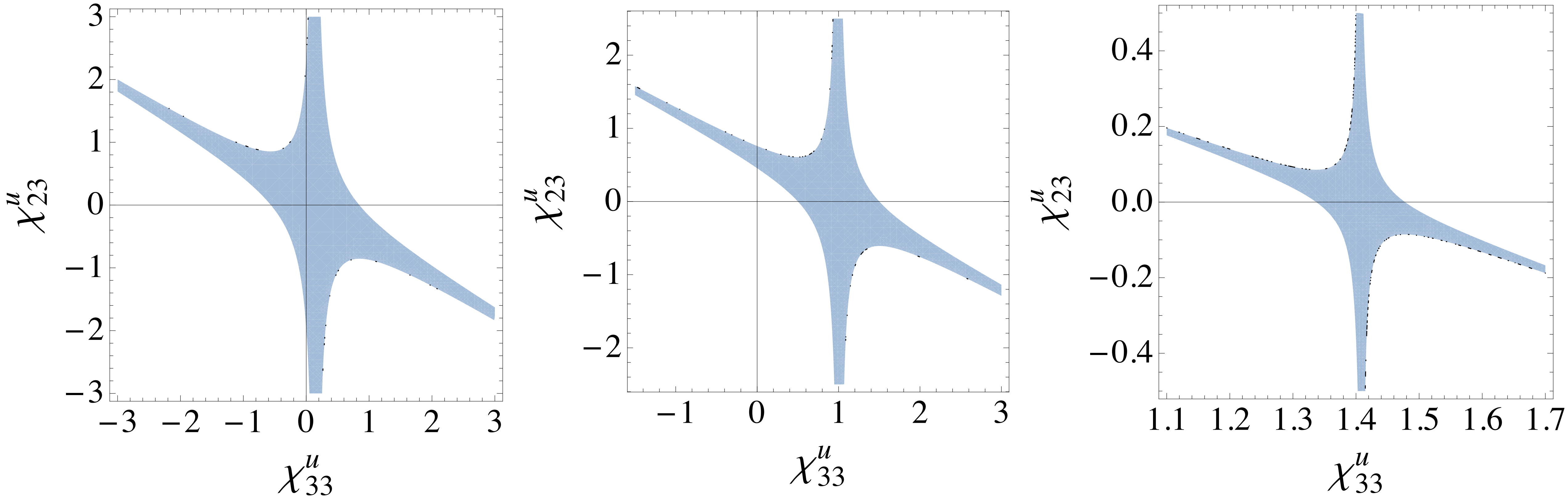

FIG. 8. The allowed region for χ^u_{33} vs. χ^u_{23} from $B \to X_s\gamma$ (using the constraint $\left|\frac{Y_{33}Y^*_{32}}{V_{tb}V_{ts}}\right| < 0.25$) and $B^0 - \bar{B}^0$ mixing (considering the constraint $\left|\frac{Y_{33}Y^*_{31}}{V_{tb}V_{td}}\right| < 0.25$) for the following cases: $|Y| << 1$ (left), $Y = 1$ (center) and $Y = 10$ (right), with $80 \text{ GeV} \leq m_{H^\pm} \leq 200 \text{ GeV}$.

13

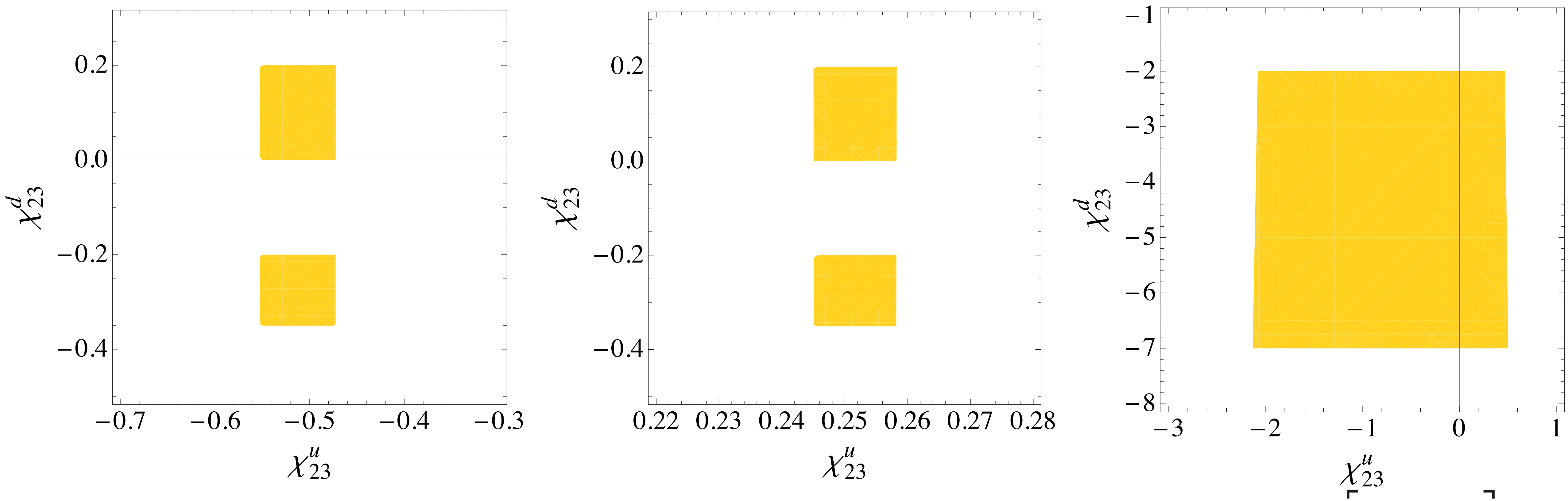

FIG. 9. The allowed region for χ^u_{23} vs. χ^d_{23} from $B \to X_s\gamma$ (using the constraint $-1.7 < Re\left[\frac{X_{33}Y^*_{32}}{V_{tb}V_{ts}}\right] < 0.7$) for the following cases: $X = 20$ and $Y = 0.1$ (left), $X = Y = 20$ (center) and $X = Y = 0.1$ (right), with 80 GeV $\leq m_{H^\pm} \leq$ 200 GeV. We assume $\chi^u_{33} = 1$, $\chi^d_{33} = 1$.

14

For light charged Higgs

$$\Gamma(H^{\pm} \to u_i d_j) = \frac{3G_F m_{H^{\pm}} (m_{d_j}^2 |X_{ij}|^2 + m_{u_i}^2 |Y_{ij}|^2)}{4\pi\sqrt{2}}$$

; the case $Y >>, X,Z$ the channel decay $H^+ \to c\bar{b}$

$$m_c Y_{cb} = m_c Y_{23} = V_{cb} m_c \left(Y - \frac{f(Y)}{\sqrt{2}} \chi_{22}^u \right) - V_{tb} \frac{f(Y)}{\sqrt{2}} \sqrt{m_t m_c} \chi_{23}^u$$

$(H^{\pm} \to cs)$

$$m_c Y_{cs} = m_c Y_{22} = V_{cs} m_c \left(Y - \frac{f(Y)}{\sqrt{2}} \chi_{22}^u \right) - V_{ts} \frac{f(Y)}{\sqrt{2}} \sqrt{m_t m_c} \chi_{23}^u$$

$$\frac{\mathrm{BR}(H^{\pm} \to cb)}{\mathrm{BR}(H^{\pm} \to cs)} = R_{sb} \sim \frac{|V_{tb}|^2}{|V_{ts}|^2}$$

For light charged Higgs

Other case is when $X >>, Y, Z$, we get the dominants terms $m_b X_{23}$, $m_s X_{22}$:

$$m_b X_{cb} \;=\; m_b X_{23} = V_{cb} m_b \left(X - \frac{f(X)}{\sqrt{2}} \chi^d_{33} \right) - V_{cs} \frac{f(X)}{\sqrt{2}} \sqrt{m_b m_s} \chi^d_{23}$$

$$m_s X_{cs} \;=\; m_s X_{22} = V_{cs} m_s \left(X - \frac{f(X)}{\sqrt{2}} \chi^d_{22} \right) - V_{ts} \frac{f(X)}{\sqrt{2}} \sqrt{m_b m_s} \chi^d_{23}$$

If $\chi = O(1)$ and positive then $\left(X - \frac{f(X)}{\sqrt{2}} \chi^d_{33} \right)$ is small and $R_{sb} \sim \frac{|V_{cs}|^2}{|V_{cb}|^2}$,

Other situation is when, $\chi = O(1)$ and negative, then $R_{sb} \sim \frac{m_b^2 |V_{cb}|^2}{m_s^2 |V_{cb}|^2}$;

A.G. Akeroyd, S. Moretti and J. Hernández-Sánchez, PRD85:115002 (2012)

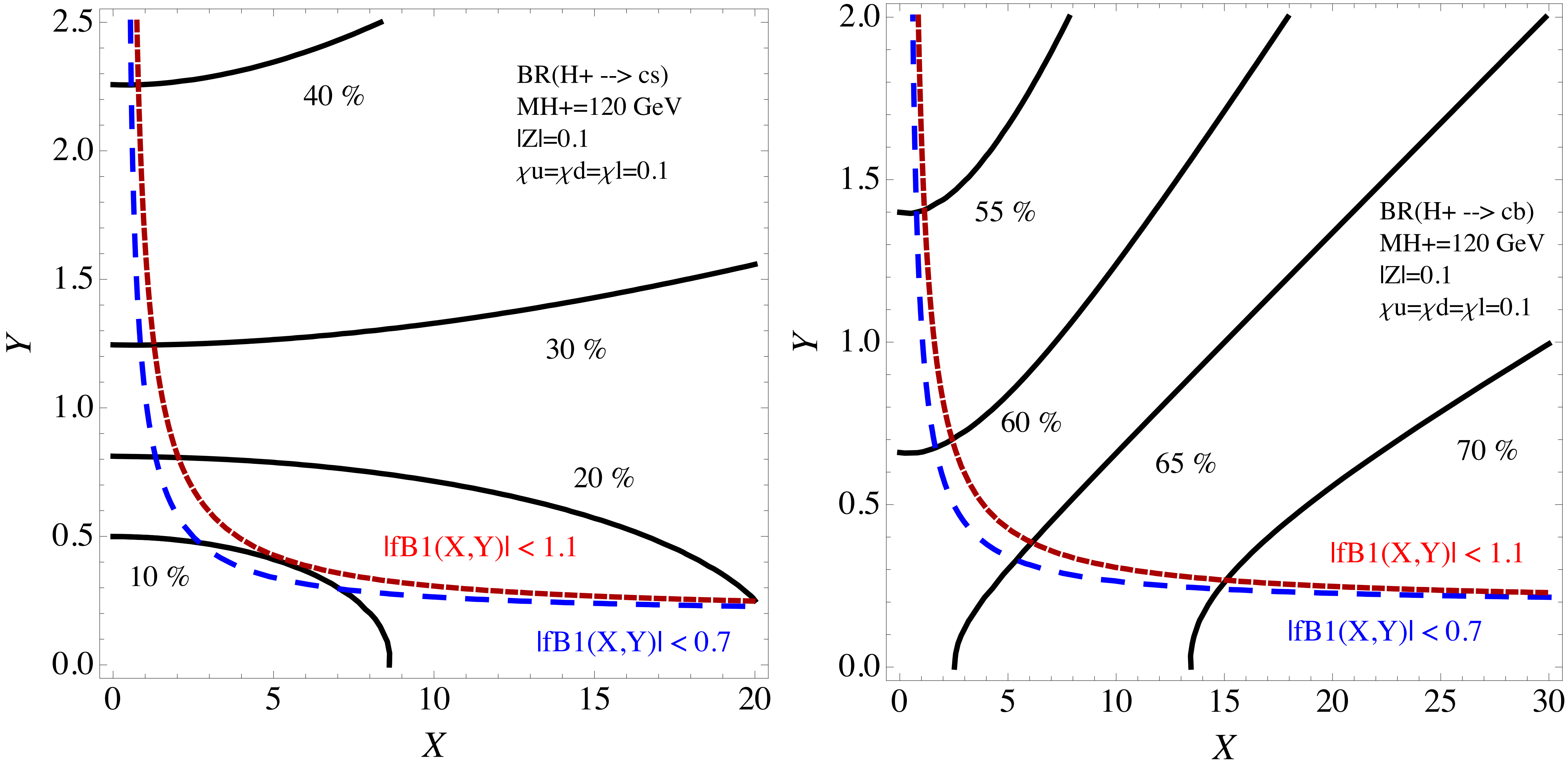

FIG. 10. For the exotic scenario of eq. (98) we show the contours of the BR($H^\pm \to cs$) (left) and BR($H^\pm \to cb$) (right) in the plane $[X, Y]$ with $Z = 0.1$, $m_{A^0} = 80$ GeV, $m_{H^\pm} = 120$ GeV and $\chi^f_{ij} = 0.1$. The constraint $b \to s\gamma$ is shown as $|fB1(X,Y)| < 1.1$ for $Re[fB1(X,Y)] < 0$, where $fB1(X,Y) = \frac{X_{33}Y^*_{32}}{V_{tb}V_{ts}}$ is given in eq. (64). For $|fB1(X,Y)| < 0.7$, it is when $Re[fB1(X,Y)] < 0$. We take $m_s(Q = m_{H^\pm}) = 0.055$ GeV.

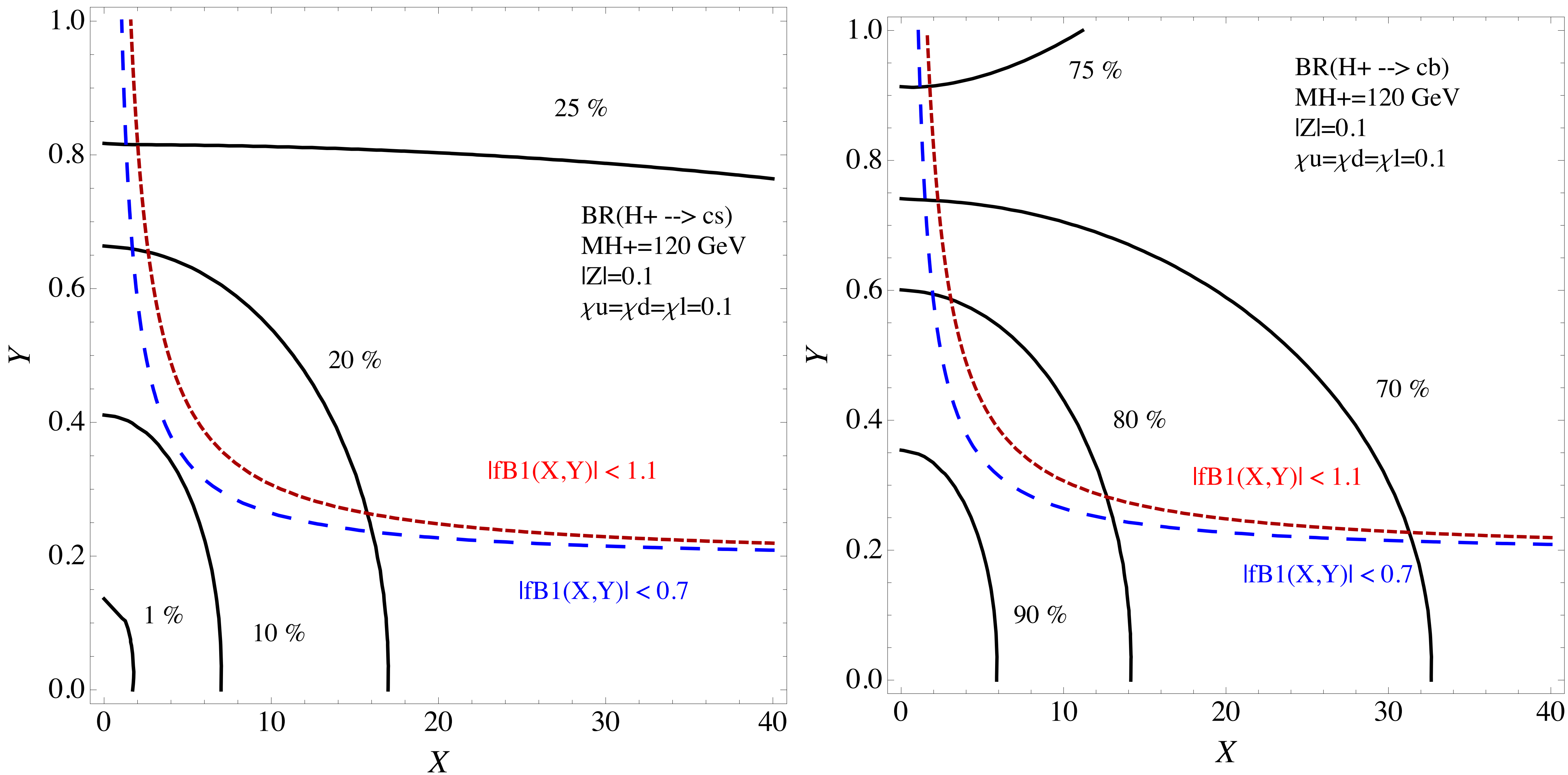

FIG. 11. The same as Fig. 10 but for $m_{A^0} = 100$ GeV.

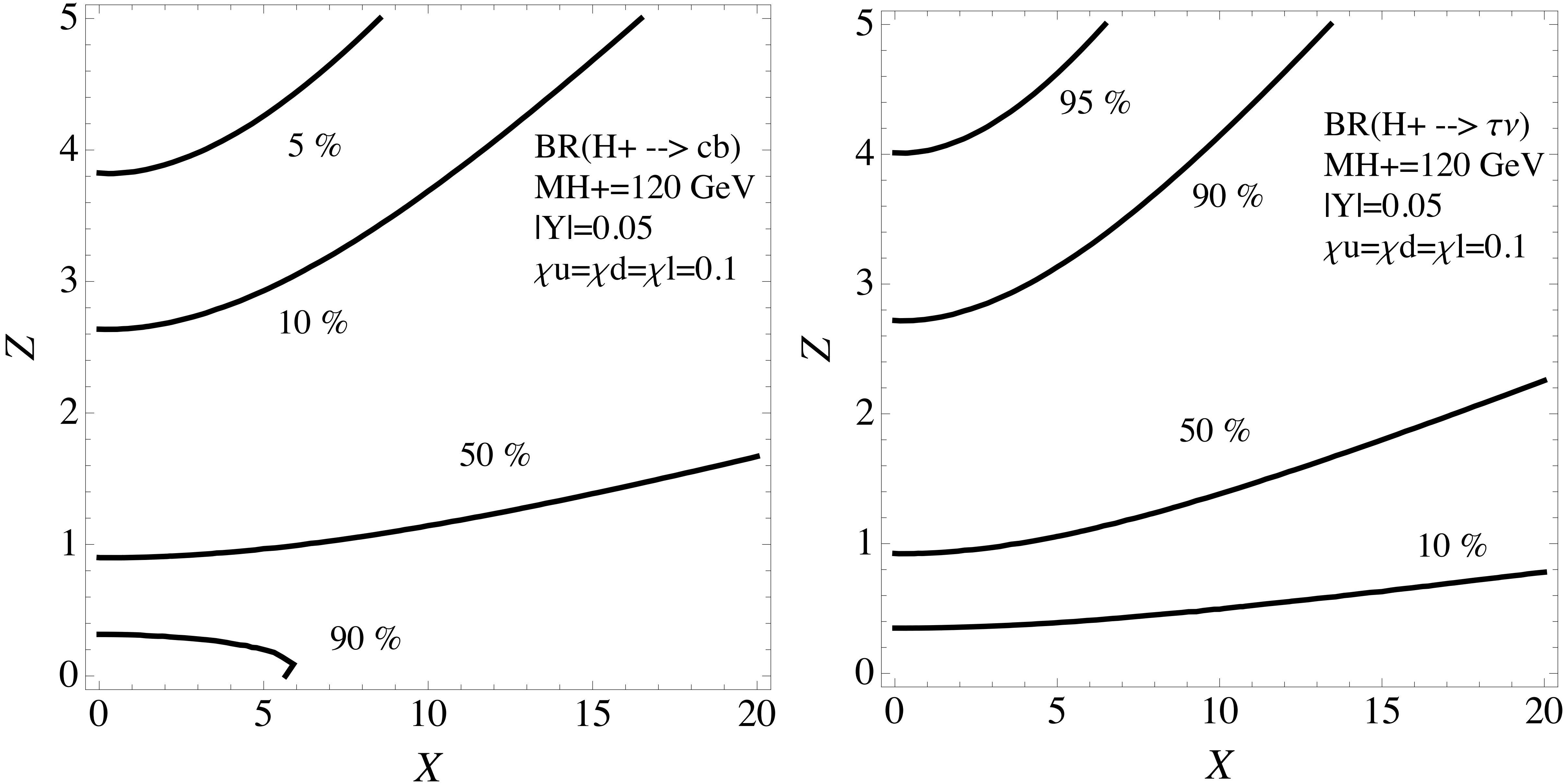

FIG. 12. For the exotic scenario of the eq. (95), we show the contours of the BR($H^{\pm} \to cb$) (left) and BR($H^{\pm} \to \tau\nu$) (right) in the plane $[X, Z]$ with $Z = 0.05$, $Z >> X$, $m_{H^{\pm}} = 120$ GeV and $\chi_{ij}^{f} = 0.1$. We take $m_s(Q = m_{H^{\pm}}) = 0.055$ GeV.

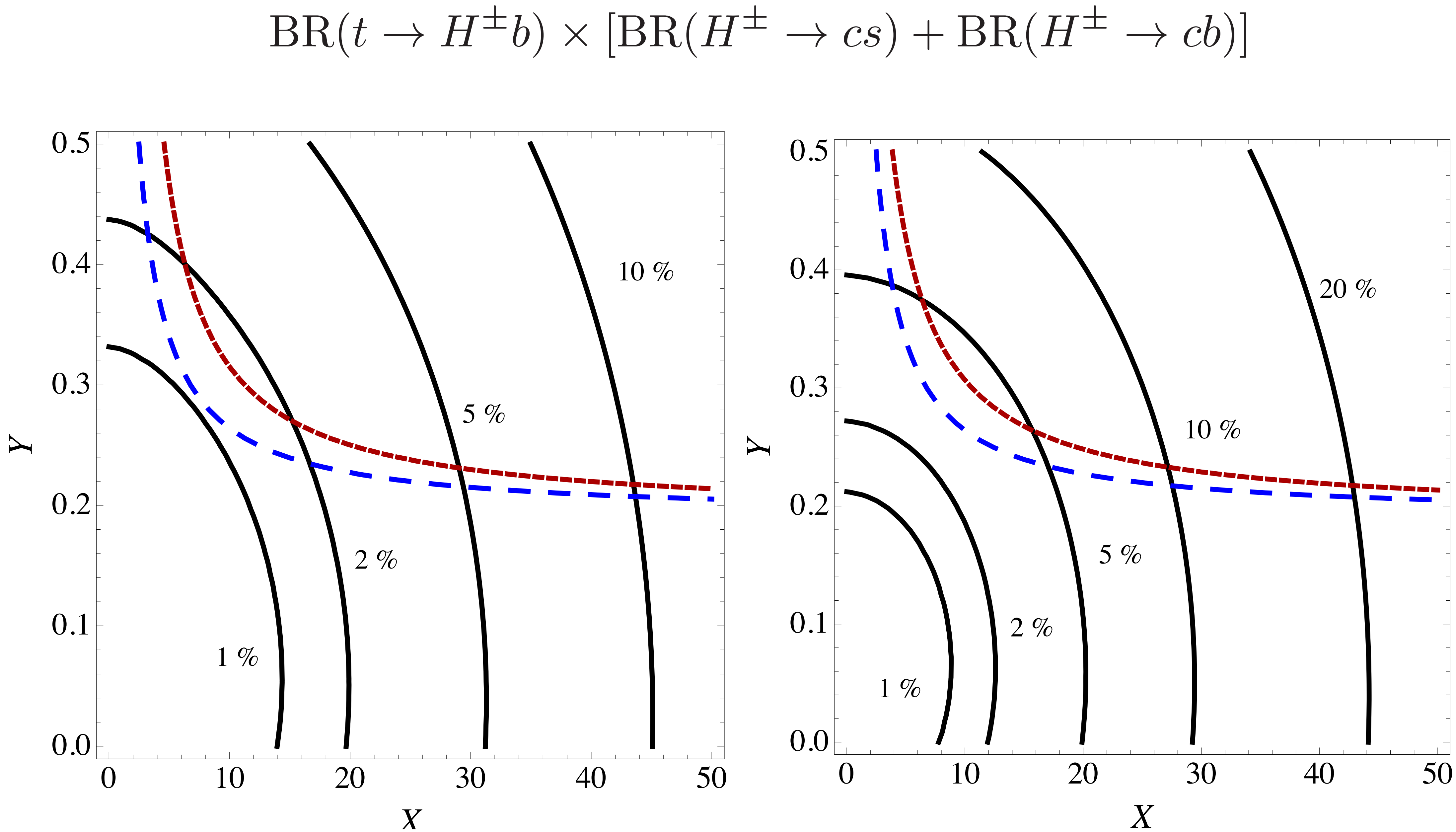

FIG. 14. Contours of the sum of $\mathrm{BR}(t \to H^\pm b) \times \mathrm{BR}(H^\pm \to cs)$ and $\mathrm{BR}(t \to H^\pm b) \times \mathrm{BR}(H^\pm \to cb)$ in the plane $[X, Y]$ with $|Z| = 0.1$, where $m_{H^\pm} = 120$ GeV (left panel) and $m_{H^\pm} = 80$ GeV (right panel).

b-tag are applied to the jets originating from t decays, but no b-tag is applied to the jets originating from H+

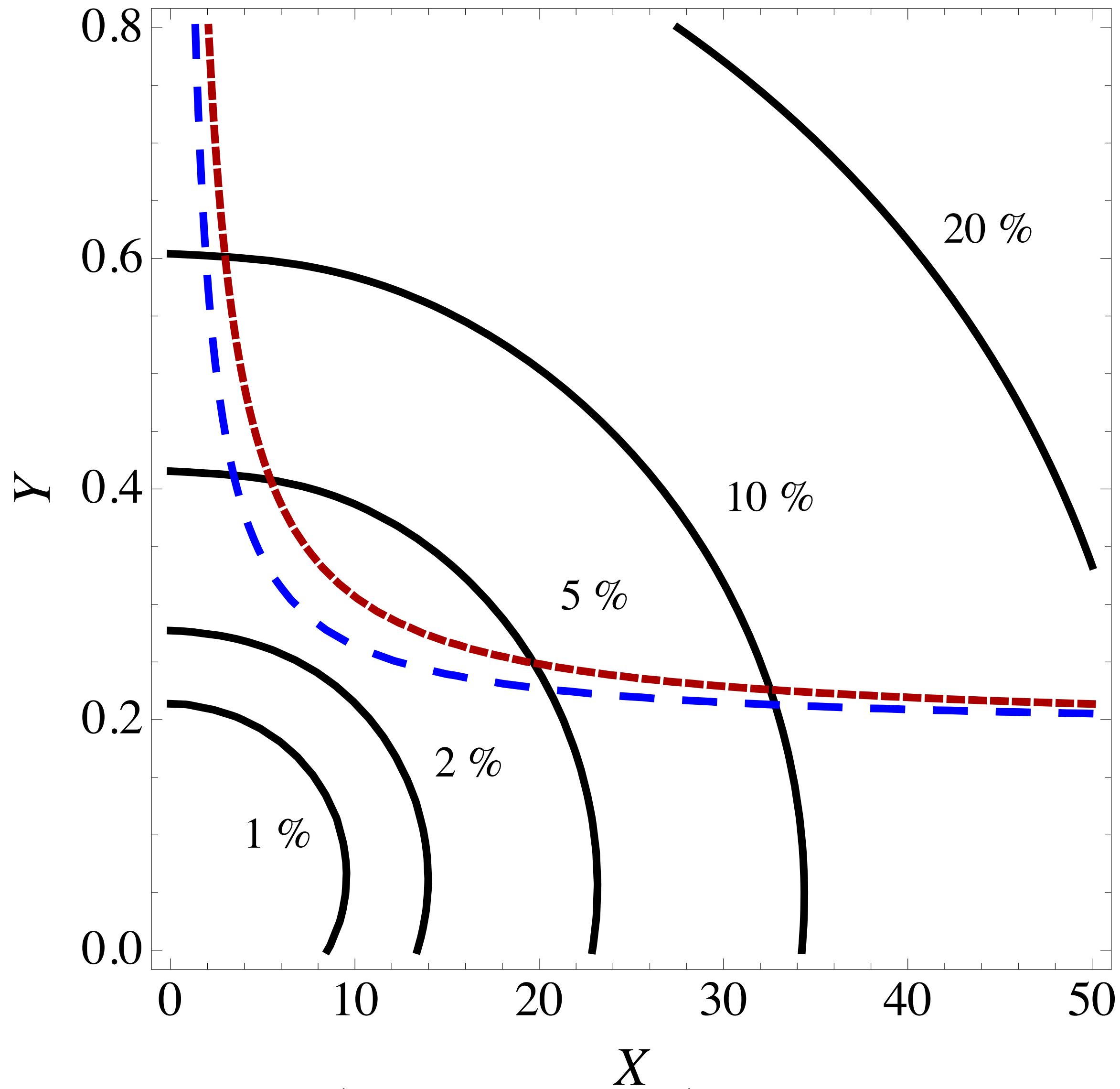

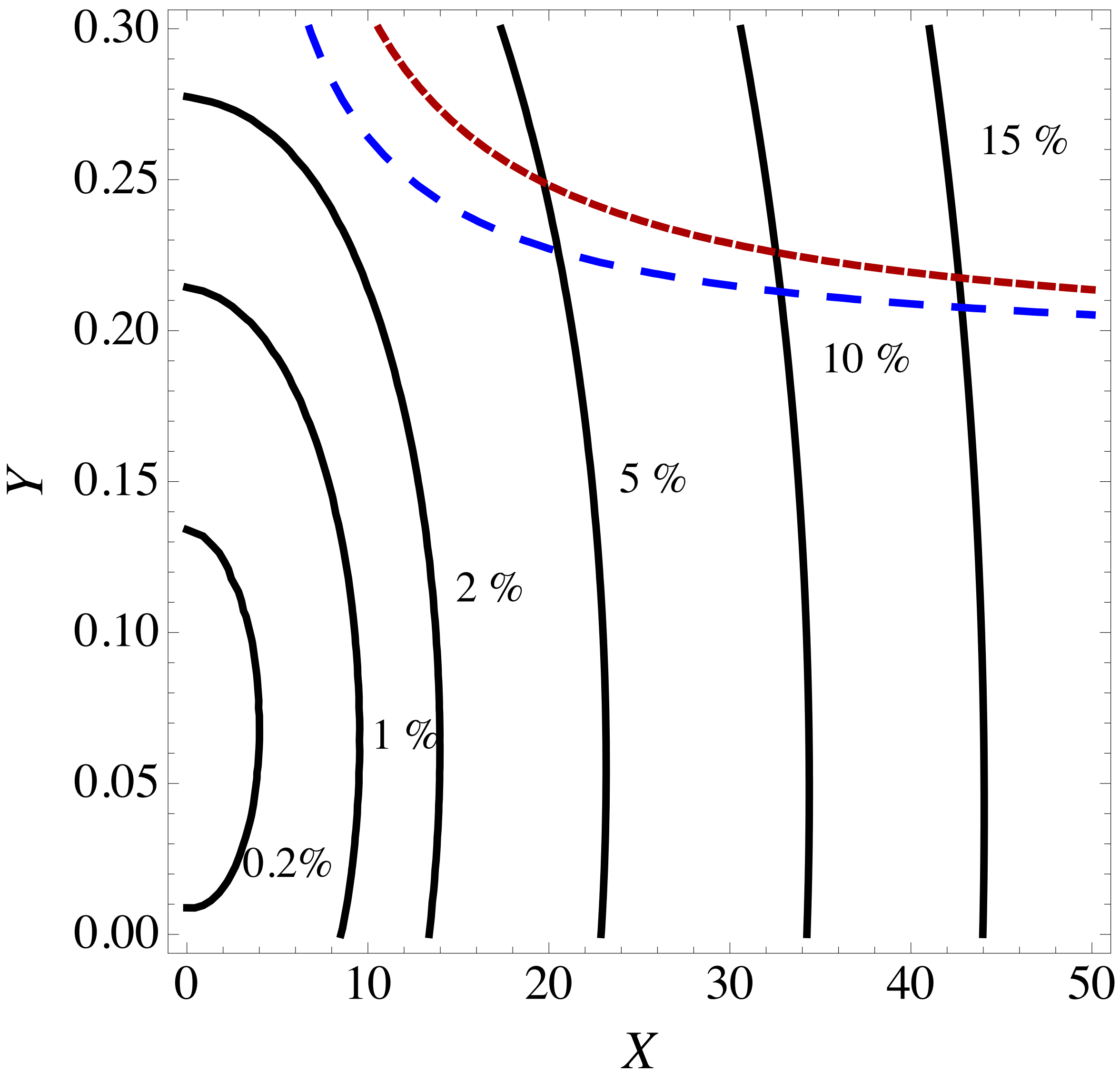

$$\mathrm{BR}(t \to H^{\pm} b) \times \mathrm{BR}(H^{\pm} \to cb)$$

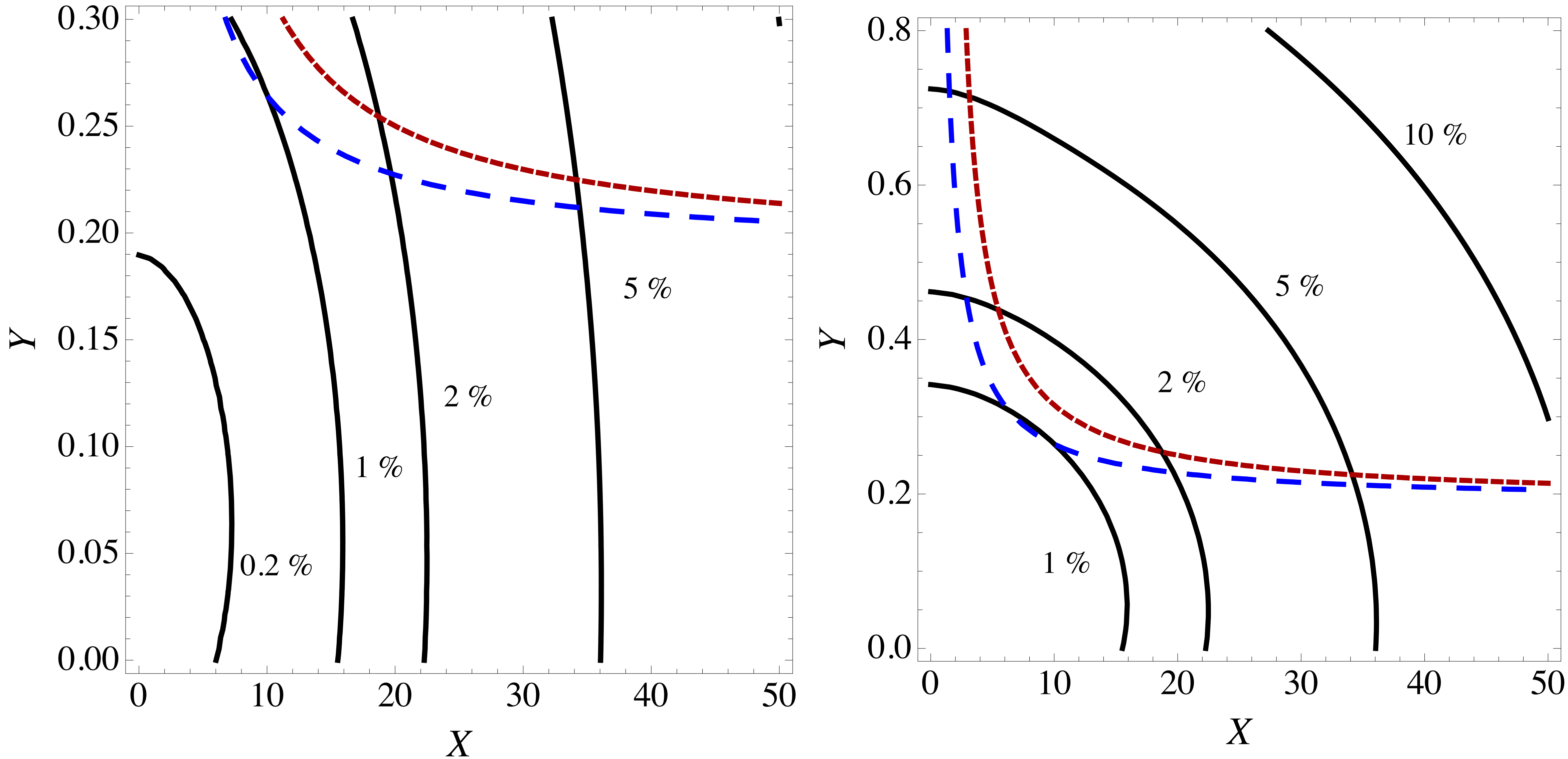

FIG. 16. Contours of BR$(t \to H^{\pm}b) \times$ BR$(H^{\pm} \to cb)$ in the plane $[X,\, Y]$ with $|Z| = 0.1$ for $m_{H^{\pm}} = 120$ GeV. The constraint $b \to s\gamma$ is shown as $|fB1(X,Y)| < 1.1$ for $Re[fB1(X,Y)] < 0$ (red-dashed), and $|fB1(X,Y)| < 0.7$ is when $Re[fB1(X,Y)] < 0$ (blue-dashed). We take $m_s(Q = m_{H^{\pm}}) = 0.055$ GeV and show the range $0 < |Y| < 0.8$ (left panel) and $0 < |Y| < 0.3$ (right panel).

22

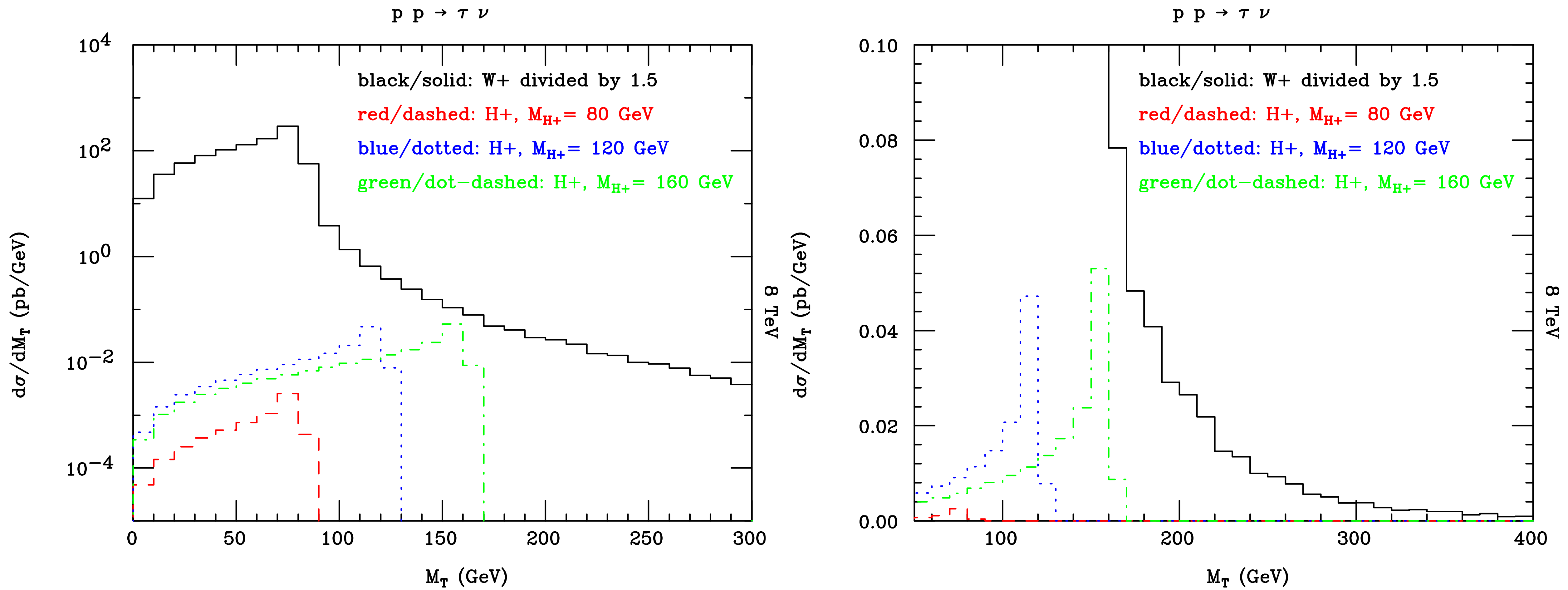

FIG. 17. Differential distributions in transverse mass M_T for signal and background (the former for three $H^{\pm}$ mass values) in logaritmic (top) and linear (bottom) scale. Here, $\sqrt{s} = 8$ TeV.

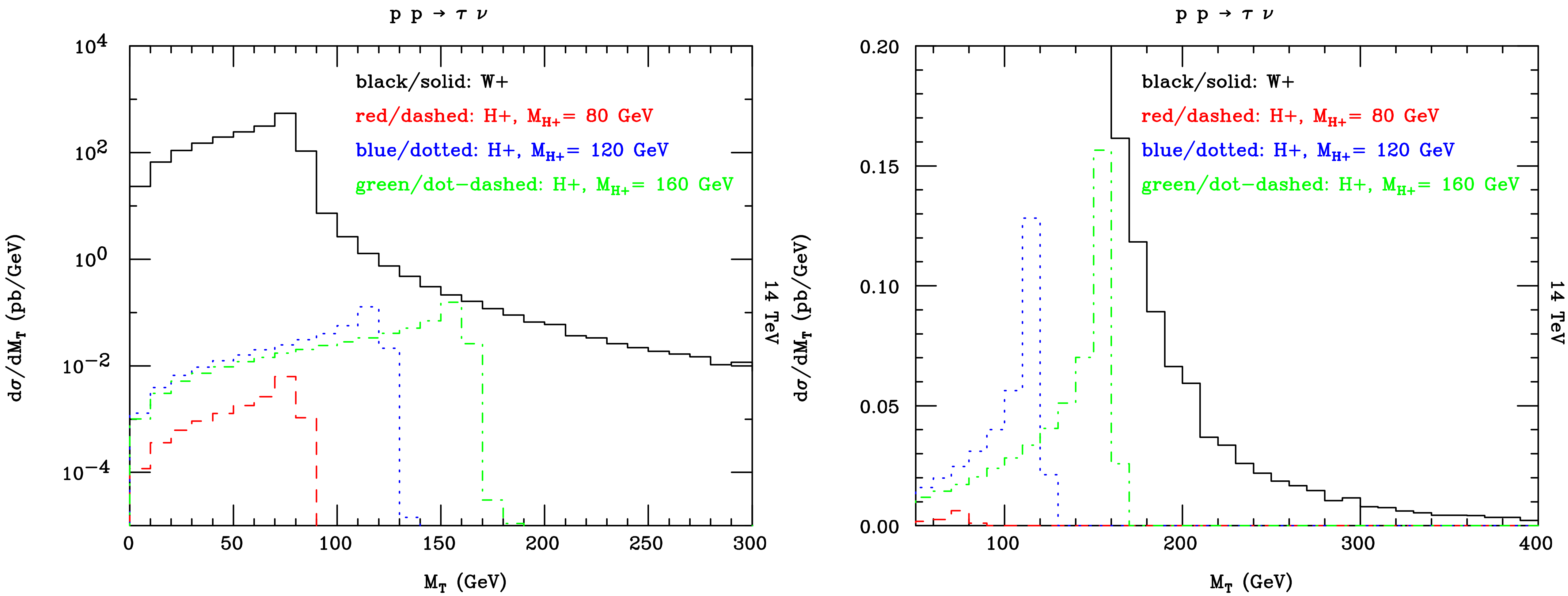

FIG. 18. The same as Fig. 17, but for $\sqrt{s} = 14$ TeV.

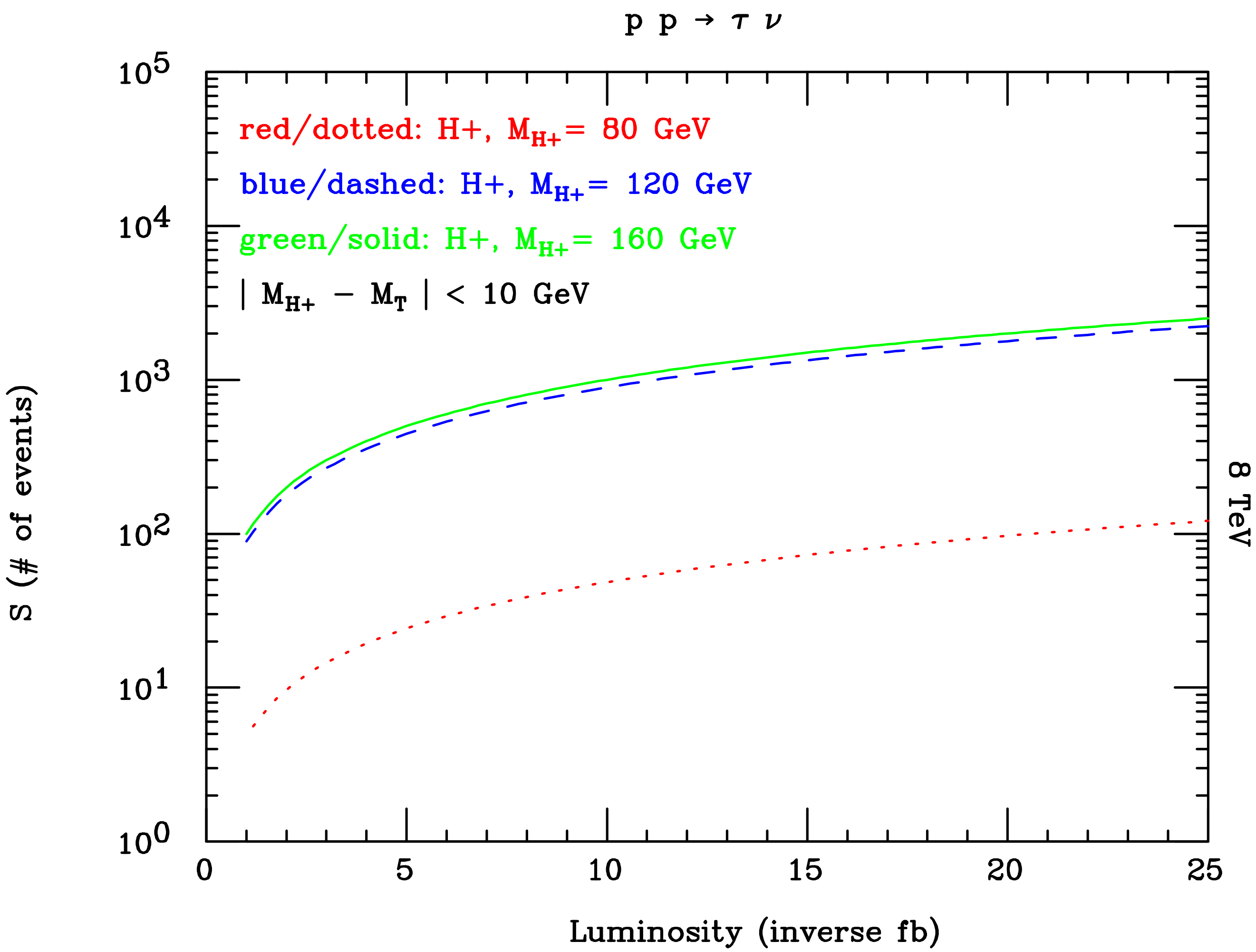
p p → τ ν
red/dotted: H+, M_H+ = 80 GeV
blue/dashed: H+, M_H+ = 120 GeV
green/solid: H+, M_H+ = 160 GeV
| M_H+ − M_T | < 10 GeV
S (# of events)
Luminosity (inverse fb)
8 TeV

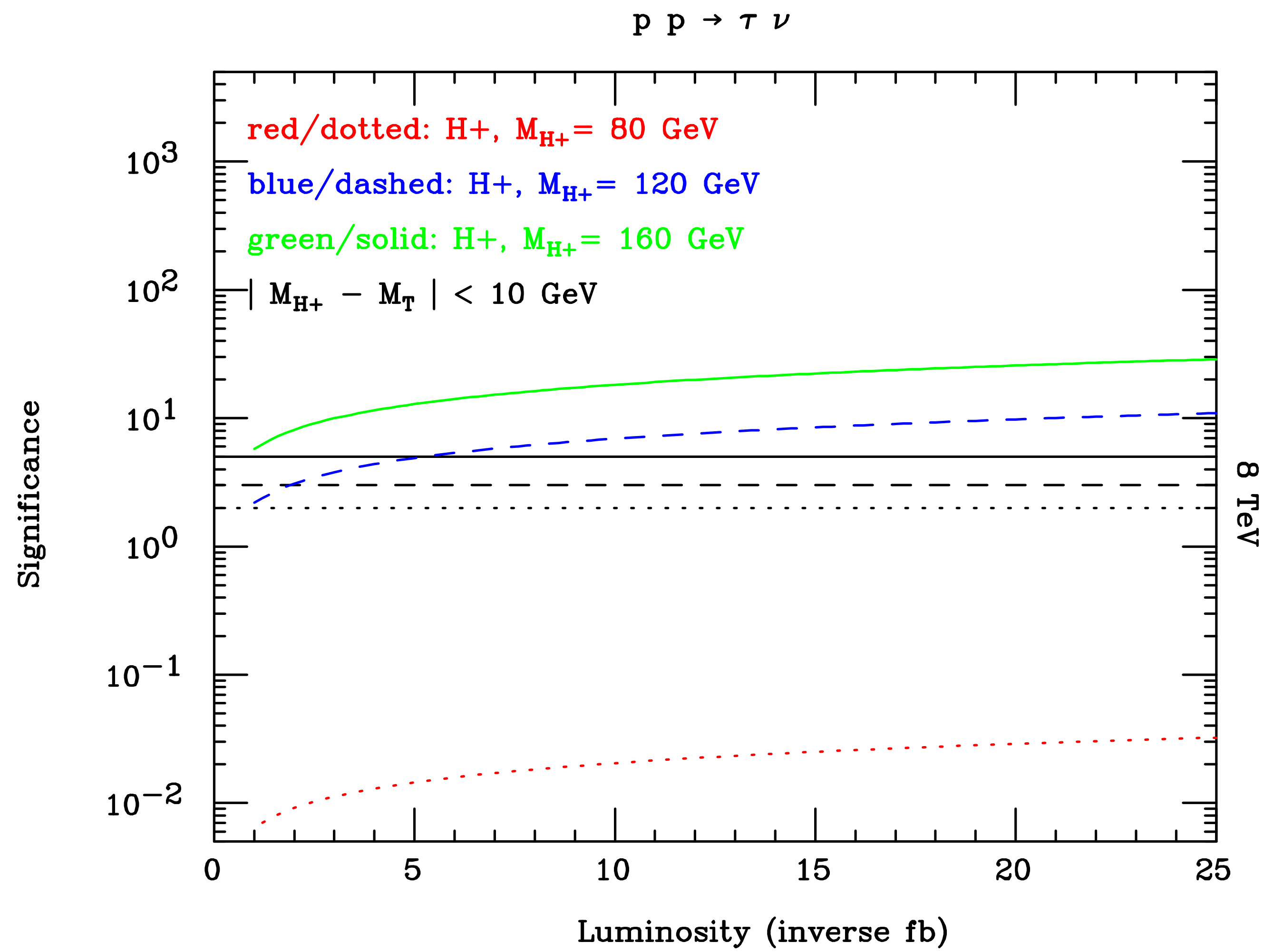
p p → τ ν
red/dotted: H+, M_H+ = 80 GeV
blue/dashed: H+, M_H+ = 120 GeV
green/solid: H+, M_H+ = 160 GeV
| M_H+ − M_T | < 10 GeV
Significance
Luminosity (inverse fb)
8 TeV

25

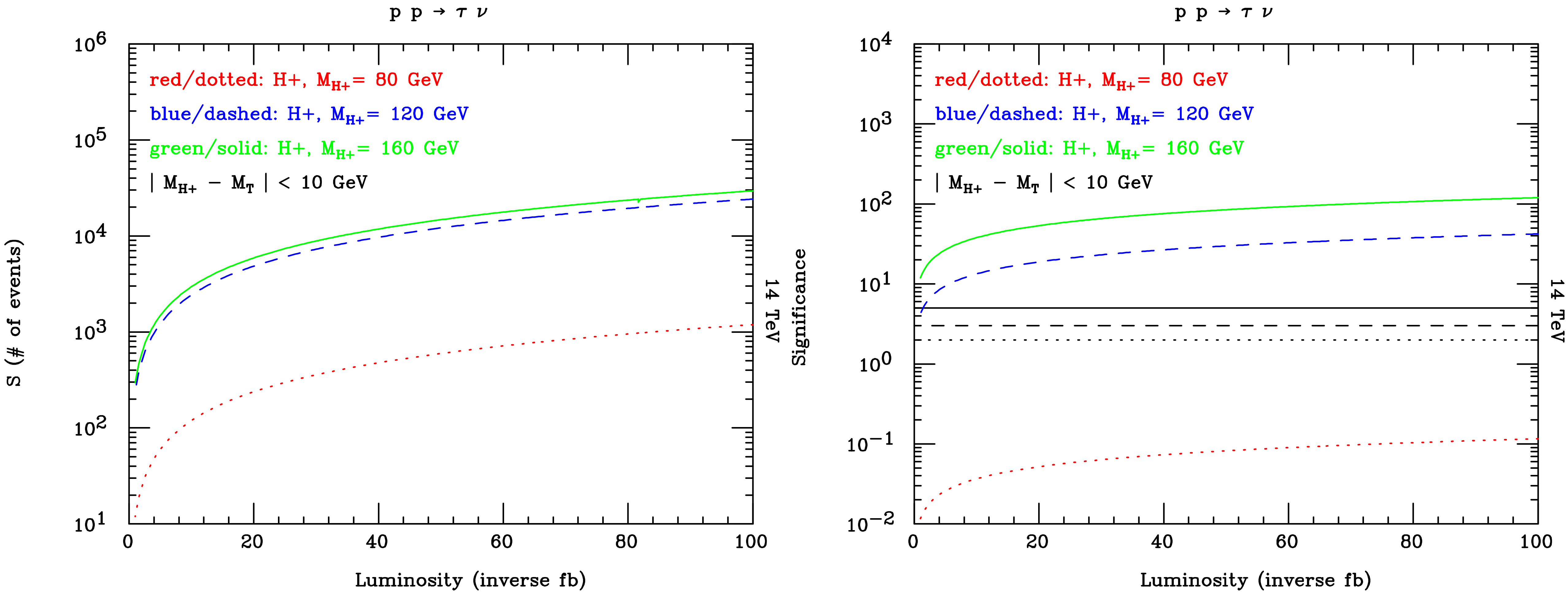

FIG. 20. The same as Fig. 19, but for $\sqrt{s} = 14$ TeV.

Others phenomenological consequences

- If we combine:

- The effects of texture in the coupling.
- The general Higgs potential.
-

It's possible to enhacement processes at one-loop-level, e.g.

- H,h→ γγ
- H^+→ W^+ γ, W^+ Z

J. Hernández-Sánchez, C. G. Honoratp, M.A. Pérez, J.J. Toscano, PRD85:015020 (2012).

J.E. Barradas, F. Cazares-Bush, A. Cordero-Cid, O. Félix-Beltrán, J. Hernández-Sanchez, R. Noriega-Papaqui, J.Phys. G37 (2010) 115008

Scenario with $\chi=1$, but $\alpha=\pi/2+\beta$

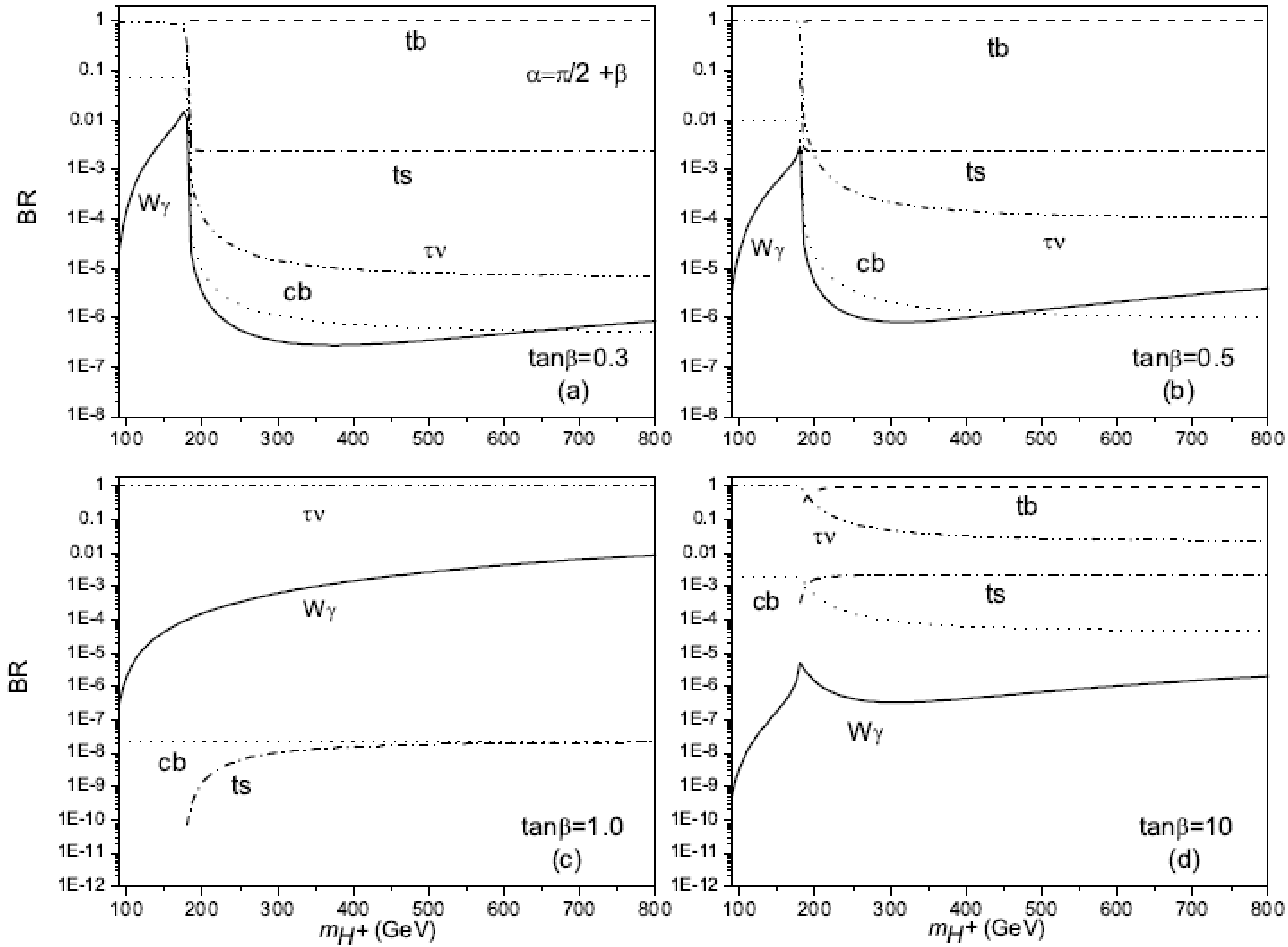

TABLE II: Summary of LHC event rates for some parameter combinations within Scenarios A, B, C, D with for an integrated luminosity of 10^5 pb^{-1}, for several different signatures, through the channel $c\bar{b} \to H^+ +$ c.c.

$(\tilde{\chi}^u_{ij}, \tilde{\chi}^d_{ij})$	$\tan\beta$	m_{H^+} in GeV	$\sigma(pp \to H^+ + X)$ in pb	Relevant BRs	Nr. Events
(1,1)	15	400	1.14×10^{-1}	$\mathrm{BR}(H^+ \to t\bar{b}) \approx 3.2 \times 10^{-1}$	3648
				$\mathrm{BR}(H^+ \to \tau^+ \nu^0_\tau) \approx 2.1 \times 10^{-3}$	24
				$\mathrm{BR}(H^+ \to W^+ h^0) \approx 6.3 \times 10^{-1}$	7182
				$\mathrm{BR}\left(H_2^+ \to W^+ A^0\right) \approx 1.7 \times 10^{-2}$	194
(1,1)	70	400	1.25×10^{-1}	$\mathrm{BR}(H^+ \to t\bar{b}) \approx 3.5 \times 10^{-1}$	4375
				$\mathrm{BR}(H^+ \to c\bar{b}) \approx 1.4 \times 10^{-2}$	175
				$\mathrm{BR}(H^+ \to \tau^+ \nu_\tau) \approx 2.5 \times 10^{-1}$	3125
				$\mathrm{BR}(H^+ \to W^+ h^0) \approx 3.6 \times 10^{-1}$	4500
(0.1,1)	1	600	3.41×10^{-4}	$\mathrm{BR}(H^+ \to t\bar{b}) \approx 3 \times 10^{-1}$	10
				$\mathrm{BR}(H^+ \to t\bar{s}) \approx 9.1 \times 10^{-4}$	0
				$\mathrm{BR}(H^+ \to W^+ h^0) \approx 3.6 \times 10^{-1}$	12
				$\mathrm{BR}(H^+ \to W^+ A^0) \approx 3.2 \times 10^{-1}$	11

Table 1. Summary of LHC event rates for some parameter combinations within Scenario B ($\tilde{\chi}^{u,d}_{ij} = 1$) with an integrated luminosity of 10^5 pb^{-1}, for the signal $H^+ \to W^+\gamma$, through the channel $c\bar{b} \to H^+$ + c.c.

α	$\tan\beta$	m_{H^+} in GeV	$\sigma(pp \to H^+ + X)$ in pb	$BR(H^+ \to W^+\gamma)$	N_S	$\frac{N_S}{\sqrt{N_B}}$
$\pi/2$	0.3	200	2.1×10^2	2×10^{-6}	42	2.02
$\pi/2+\beta$	0.5	300	4.5×10	9×10^{-7}	4	0.223
$\pi/2$	1	200	4.5	1.4×10^{-4}	63	3.03
$\pi/2+\beta$	1	300	0.89	7×10^{-4}	62	3.46
$\pi/2$	10	200	2.5	2×10^{-6}	0	0
$\pi/2$	10	300	5.2×10^{-1}	1.5×10^{-7}	0	0

Conclusions

- 2HDM-III with a four-zero texture in the Yukawa matrices could contain the versions of 2HDM.
- The terms off-diagonal matrices Xij could be O(1) and cannot omitted, including some important constraints of processes to low energy.
- H+ → cb could be relevant.
- H+ → W+ gamma could enhance.
- Production H+ could be quite different to the results of the others versions of 2HDM.